ELSEVIER

Catalysis Today 40 (1998) 353–365

CATALYSIS TODAY

Relationship between the formation of surface species and catalyst deactivation during the gas-phase photocatalytic oxidation of toluene

Rafael Méndez-Román, Nelson Cardona-Martínez*

Department of Chemical Engineering, University of Puerto Rico – Mayagüez Campus, Mayagüez 00681-9046, Puerto Rico

Abstract

Various partial oxidation products were identified on the surface of TiO_2 and an 8% SiO_2–TiO_2 binary catalyst used for the photocatalytic oxidation of gas-phase toluene. Using in situ FTIR spectroscopy, benzaldehyde and benzoic acid were identified on the surface of the deactivated photocatalysts. Additional GC/MS analysis of methanol-extracted surface species confirmed the presence of benzaldehyde and benzoic acid and detected small concentrations of benzyl alcohol. Apparently, benzaldehyde is the main partial oxidation product that is further oxidized to benzoic acid. Benzoic acid is strongly adsorbed on the surface of the catalyst. There seems to be a correlation between the accumulation of benzoic acid on the surface and catalyst deactivation. The presence of gas-phase water in the reactive mixture seems to retard the formation of benzoic acid.

The SiO_2–TiO_2 photocatalyst is more active and appears to deactivate slower than TiO_2. This binary oxide is photocatalytically active even in the absence of gas-phase oxygen. It also seems to have a higher toluene adsorption capacity than TiO_2. The acidity of the different oxides was examined using FTIR spectroscopy of adsorbed pyridine. The results indicate that no pure metal oxide displays Brønsted acidity but when SiO_2 is cofumed with TiO_2, Brønsted acidity of intermediate strength is generated. The generation of new surface sites may be responsible for the increased activity. The mechanism of this promotion effect is not clearly understood and further studies are required to elucidate it.

Keywords: Photocatalysis; Toluene oxidation; Deactivation; FTIR spectroscopy; Titania; Silica–titania; Pyridine adsorption

1. Introduction

Excitation of a photocatalyst leads to the creation of electrons and holes in the semiconductor (e.g., [1–3]). These electrons and holes interact with molecules adsorbed on the semiconductor and can induce charge transfer processes that ultimately may result in the degradation of the adsorbate. The use of photocatalysis for the abatement of environmental problems has received increased attention during the last decade. Recent reviews summarize many of these studies (e.g., [1–4]). The photocatalyst used in most of these studies was TiO_2. Initially, the emphasis was on the application of photocatalysis for water treatment. After the discovery that the photocatalytic detoxification of volatile organic compounds (VOCs) is generally more efficient in the gas phase than in the liquid phase (e.g., [5–9]), and more importantly, that the treatment cost may be significantly lower than that of the water-phase photocatalytic treatment or the use of conventional treatment technologies [10,11], the emphasis has

*Corresponding author. Fax: 00787-265-3818; e-mail: ne_cardona@rumac.upr.clu.edu.

0920-5861/98/$32.00
PII S0920-5861(98)00064-9

shifted towards the application of photocatalysis for air treatment.

Toluene is a major indoor and industrial air pollutant. Various studies have tested the potential use of gas-phase photocatalytic oxidation of toluene for air detoxification [12–18]. However, there are still issues unanswered for the effective implementation of gas-phase photocatalytic technology at a commercial level for the oxidation of toluene or other contaminants. Some of these topics include: (1) catalyst deactivation, (2) the formation of byproducts and their fate, and (3) the enhancement in activity caused by supports or secondary oxides. The work presented here addresses all these issues.

1.1. Photocatalyst deactivation

A recent survey of the literature on photocatalytic air treatment and purification accentuated the emerging photocatalyst deactivation issue [19]. A comparison among the results reported demonstrated that catalyst deactivation was observed for single-pass fixed bed reactor's studies that achieved contaminant conversions of at least one surface monolayer equivalent. The authors defined the surface monolayer equivalent as the cumulative reactant conversion divided by the number of active catalyst sites (molecules converted per active catalyst site). These results imply that the photocatalysts are deactivated by accumulation of surface species formed during the reaction. Deactivation was reported for various compounds. Different hypotheses have been given to explain the deactivation process. Cunningham and Hodnett [20] suggested that the CO_2 formed during the oxidation of alcohols adsorbed on the TiO_2 catalyst surface and competed for the catalyst active sites. It is unlikely that adsorbed CO_2 causes the deactivation because all photocatalyzed oxidations of carbon containing reactants produce CO_2, but deactivation has been reported for only some reaction systems. Peral and Ollis [21] noted catalyst deactivation when photooxidizing 1-butanol or butyraldehyde. These authors proposed that the formation of strongly adsorbed butanoic acid in both cases was responsible for the catalyst deactivation. The deactivation of TiO_2 during the gas-phase photooxidation of trichloroethylene was reported by Larson and Falconer [22]. These researchers indicated that apparently strongly bound species, such as carbonates, accumulated on the surface deactivating the catalyst. Jacoby et al. [23] observed catalyst deactivation during the photocatalytic oxidation of benzene on TiO_2. Identification of polar intermediates adsorbed on the catalyst surface was investigated through water extraction of the deactivated catalyst followed by analysis via high performance liquid chromatography. The provisional identification detected phenol, malonic acid, and hydroquinone and/or benzoquinone as surface-bound intermediates, but no suggestion was given to explain the deactivation.

Catalyst deactivation for the photocatalytic oxidation of toluene and toluene mixed with trichloroethylene, trichloropropene or perchloroethylene has been reported by Ollis and coworkers [12,13]. Extraction of the adsorbed species followed by mass spectrum analysis indicated the major adsorbed intermediate to be benzoic acid. Again, carboxylate formation and carboxylic acid accumulation were postulated as a major cause of catalyst deactivation. Using temperature-programmed oxidation and desorption, Larson and Falconer [14] indicated that the first step in the photocatalytic oxidation of benzene, toluene, *p*-xylene, and mesitylene form less-reactive intermediates. These species are much more strongly bound to TiO_2 than the original aromatic compounds and are expected to deactivate the catalyst. According to their results, the less-reactive intermediates did not appear to be aldehydes or alcohols. Benzoic acid was suggested as the possible cause of the deactivation but was not tested. Most aromatic hydrocarbon photocatalytic oxidation studies do not report gas-phase intermediates, but trace level benzaldehyde has been detected during the photocatalytic oxidation of toluene [15,16]. The characterization of intermediate products involved in the degradation of VOCs is central to any research program aimed at the development of new technologies suitable for the abatement of environmental problems. These products are important because we do not want to convert VOCs into more reactive or hazardous compounds. Rather, their degradation into simple molecules is desired. It has been demonstrated above that intermediate products that are retained on the surface can lead to a number of problems that include catalyst deactivation.

The amount of water present, both on the surface and in the gas phase, has a strong influence on the

photocatalytic activity and selectivity of TiO_2. The dependence of water vapor concentration on the photocatalytic oxidation rate is complex. According to Ibusuki and Takeuchi [15] water vapor is required for toluene oxidation. These authors found no conversion in the absence of water vapor and that the photooxidation rate increased linearly with increasing relative humidity over the range 0–60%. Obee and Brown [17], on the other hand, found that the toluene oxidation rate passed through a maximum when the water concentration was increased. Apparently, at high water concentrations, an inhibition effect is caused by competitive adsorption between water and toluene. Both results are consistent with a solar pilot-plant study [16]. The water vapor content can also drastically alter the distribution of products. For example, for the photocatalytic oxidation of trichloroethylene, increasing the water vapor concentration from 0% to 3% increased the production of CO and HCl and decreased the production of $COCl_2$ and Cl_2 [9]. In the complete absence of water vapor, the catalyst photooxidation activity rapidly declines with time on stream [6,16]. When water is present in the reactive mixture the decrease in activity is slower [16]. Catalyst activity may be completely or partially recovered (depending on the reactive system) by flowing humid air over the catalyst in the presence of UV illumination. The influence of water in catalyst regeneration and on the rate of reaction remains unclear and strongly depends on other operational variables. Further catalyst deactivation (and regeneration) studies in gas–solid photocatalysis are necessary to obtain a more detailed understanding of these processes and to establish the process economics of this technology [19].

1.2. Effect of supports or binary oxides

The efficiency of TiO_2 may be improved by reducing the recombination of the photogenerated electrons and holes by increasing the rate of transfer of these species to the reactants. The scavenging of holes may be promoted by enhancing the adsorption of the organic molecule and any partially oxidized intermediates by incorporating more effective adsorption sites than those present on the TiO_2 surface [24]. Therefore, the photocatalytic activity may be modified by supporting TiO_2 on different types of materials. For example, Anderson and Bard [24] found that a TiO_2/SiO_2 photocatalyst with a ratio of 30/70 enhances the activity for liquid-phase photocatalytic decomposition of rhodamine-6G by about three times when compared to conventional Degussa P-25 TiO_2. Xinazhi et al. [25] found that modification of titania with silica and zirconia improved the photocatalytic performance for ethylene oxidation. Takeda and coworkers [26] found that the photocatalytic activity for the photodecomposition of gaseous propionaldehyde increased when TiO_2 was supported on alumina, silica, mordenite, ferrierite, or activated carbon and decreased when X or A zeolites were used as supports. The photocatalytic activity displayed a volcano type dependence with the adsorption equilibrium constant of the TiO_2-supported catalysts. This behavior implies that a support with an intermediate affinity towards the selected organic molecule is required to obtain the highest activity.

The experimental program used in this study was designed to attempt to establish the relationship between the formation of partial oxidation products that are retained on the surface and catalyst deactivation for both TiO_2 and an 8% silica–titania binary oxide. In this work we have investigated the adsorption and photocatalytic oxidation of toluene, benzaldehyde, benzyl alcohol, and benzoic acid. In situ Fourier transform infrared (FTIR) spectroscopy was used to identify surface species formed during the oxidation of gas-phase toluene. Analysis with GC/MS of methanol-extracted surface species from the deactivated catalysts was used to confirm the formation of those species.

2. Experimental

2.1. Catalysts

The catalysts studied, P-25 TiO_2 and 8% SiO_2–TiO_2, were samples provided by Degussa and were used without further modifications. The oxides were prepared by high-temperature hydrolysis of the corresponding metal chlorides [27]. Silica (Cabot) was used for comparison. Titanium dioxide P-25 was characterized by the manufacturer as having an average particle size of about 21 nm and a specific surface area of around 50 m^2/g [28]. Approximately 70% of P-

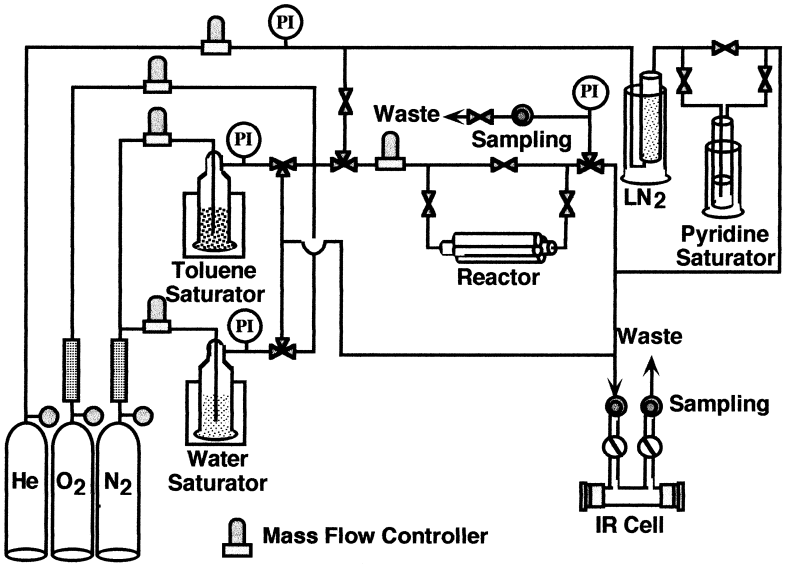

Fig. 1. Schematic of reaction and adsorption system.

25 has the anatase crystal structure and the remainder the rutile structure. The binary oxide sample was prepared by cofuming the Si and Ti chlorides and contains 8 wt% SiO_2 and 92 wt% TiO_2 P-25. This sample was also characterized by the manufacturer as having a specific surface area of around 50 m^2/g.

2.2. *Flow apparatus and sample pretreatment*

The adsorption of the organic compounds and the formation of surface species during the photocatalytic oxidation of the compounds was studied by in situ FTIR spectroscopy. A conventional flow system was used to treat the samples, to adsorb the organic compounds, or to perform the photocatalytic reaction. A schematic representation of the reaction and adsorption system is shown in Fig. 1.

Mass flow controllers (Brooks 5850E) were used to establish the flows of the different gases used. Various saturators placed in constant temperature baths were used to control the composition of the reactive or adsorptive mixtures. An in situ FTIR cell was used for analysis of the photocatalysts surface. A single-pass fixed bed reactor is also available for kinetics studies, but here we concentrate on the FTIR spectroscopy results. The Pyrex cell used to collect all spectra has a 25 mm diameter, is 150 mm long, and has 32 mm CaF_2 windows connected with Ultratorr fittings (PR Valve and Fittings). All infrared spectra were taken at room temperature with a Nicolet Magna 550 Fourier Transfer Infrared Spectrometer. For selected experiments, a Shimadzu 17A gas chromatogragh (GC), with a flame ionization detector and a 30 m capillary column (J&W DB-5), was used for analysis of the gaseous hydrocarbon products and the reactive mixture.

In a typical experiment, about 50 mg of the sample was pressed into a self-supported 1 cm wafer. The disk was placed in the sample holder and then pretreated with one of the two procedures depending on the type of experiment. For adsorption experiments, the samples were treated at 623 K in flowing helium (120 cm^3/min) for 2 h. For photocatalysis experiments the samples were treated at 623 K in flowing oxygen (40 cm^3/min) for 1 h, followed by treatment at 623 K in flowing helium (120 cm^3/min) for 1 h. After the activation, the sample was cooled to room temperature, exposed to a flow of water in nitrogen (about 5800 ppm water and 100 cm^3/min) for 1 h, and then flushed at room temperature with flowing He (120 cm^3/min) for 1 h. Helium was purified by passage through a molecular sieve (3A) trap at 77 K. Oxygen and nitrogen were purified with molecular sieve (3A)-anhydrous $CaSO_4$ (W.A. Hammond Drier-

ite) traps at room temperature. The treatment with oxygen or helium was to clean the surface and the treatment with water was an attempt to obtain a constant surface water concentration. Following the pretreatment, an initial spectrum was collected. This spectrum was subtracted from the subsequent spectra to show only the bands corresponding to the adsorbed species.

2.3. FTIR spectroscopy of adsorbed pyridine

Infrared spectroscopy of adsorbed pyridine was used to determine the types of acid sites present on the samples. The spectral region from 1400 to 1650 cm^{-1} is particularly important for acidity characterization since this range contains IR absorption frequencies expected for coordinated pyridine, pyridinium ion, and H-bonded pyridine.

Pyridine was adsorbed on the catalysts by passing a pyridine saturated helium stream through the cell at 473 K for 1 h. The pyridine (E.M. Science, 99.92% purity) saturator was placed in a constant temperature bath kept at 273 K to produce a vapor pressure of about 4.8 Torr (1 Torr=133.3 Pa). After the adsorption period, the gas-phase pyridine and any weakly adsorbed pyridine were removed from the cell by flowing helium (120 cm^3/min) for 1 h at 473 K before cooling to room temperature and collecting a spectrum. The procedure for the identification of the acid types present is straightforward and has been described for samples equilibrated with a high pyridine pressure and subsequently evacuated at increasing temperatures [29–33].

2.4. Adsorption of toluene, benzaldehyde, benzyl alcohol, and benzoic acid

Infrared spectroscopy of adsorbed toluene, benzaldehyde, benzyl alcohol, and benzoic acid was used to identify the potential intermediates formed during the photocatalytic oxidation of toluene. The spectral region from 1150 to 1750 cm^{-1} is important for identification of aromatic compounds, aldehydes, alcohols, and carboxylic acids (e.g., [34–36]).

Toluene was adsorbed on the catalysts by passing a toluene saturated nitrogen stream through the cell at 300 K for 1 h. The toluene (Fisher Scientific, 99.8% purity) saturator was placed in a constant temperature bath kept at 273 K to produce a constant vapor pressure. After the adsorption period, the gas-phase toluene and any weakly adsorbed toluene were removed from the cell by flowing helium (120 cm^3/min) for 1 h at 300 K, and a spectrum was collected. The sample was subsequently irradiated with a 100 W UV lamp (BlackRay B100AP, 365 nm) while flowing helium (80 cm^3/min). Spectra were collected after 1,2,4,6, and 8 h of irradiation.

Benzaldehyde and benzyl alcohol were adsorbed on the catalysts by injecting with a syringe between 5 and 10 μl of liquid to the cell while flowing He (120 cm^3/min) at 300 K for 15 min. After this time the needle was removed from the septum and the He flow maintained for 15 min before collecting a spectrum. Since benzoic acid is a solid at room temperature and its sublimation temperature is 373 K, we modified the adsorption procedure for this compound. For these experiments the IR cell was opened after the pretreatment and a small amount of benzoic acid (between 1 and 2 mg) was quickly placed inside the cell. A flow of He (120 cm^3/min) was immediately established and the cell was heated to 373 K. The He flow was kept for at least 15 min after no solid benzoic acid was observed. This procedure was followed by collecting a spectrum at room temperature. The three adsorbed compounds were irradiated in flowing dry air to test their reactivity.

2.5. Photocatalytic oxidation of toluene

The photocatalytic oxidation of toluene was studied in situ in the IR cell. Appropriate mixtures of toluene and water in nitrogen were mixed with oxygen and diluted in helium to obtain the desired compositions. Samples of the reactive mixture were analyzed with the GC to confirm that the desired ratios were achieved. Toluene concentrations between 30 and 200 ppm and water concentrations of 0 or 1200 ppm were used. The O_2 to N_2 ratio was the same as in air. Various gas samples were taken during the reaction for GC analysis. The reaction was continued until the catalyst deactivated as ascertained by the product analyses. Infrared spectra were collected after 1,2,4,6,8, and in some instances after 16 h of irradiation. To collect the spectra the lamp was turned off, the flow of reactive mixture stopped, and the reactor was

purged with He (120 cm^3/min) at 300 K for 1 h to remove any gas-phase products.

The deactivated catalysts were suspended in 2 ml of methanol in a dark vial to extract any adsorbed species, and the resulting solution was examined by GC mass spectrometry (MS) with a HP 6890/5973 GC/MS/DS with a HP Innowax Column (15 m× 0.25 mm).

3. Results and discussion

3.1. FTIR spectroscopy of adsorbed pyridine

The acidity of the different oxides was examined using FTIR spectroscopy of adsorbed pyridine. The infrared spectra of pyridine adsorbed at 473 K on the fresh oxides are shown in Fig. 2. The spectrum for pyridine adsorbed on silica shows only two small bands at 1598 and 1446 cm^{-1} corresponding to hydrogen-bonded pyridine [29–33]. When pyridine is adsorbed over TiO_2, four bands are observed at 1606, 1575, 1492, and 1445 cm^{-1} characteristic of aromatic ring vibrations for pyridine adsorbed on Lewis acid sites. These acid sites have been associated

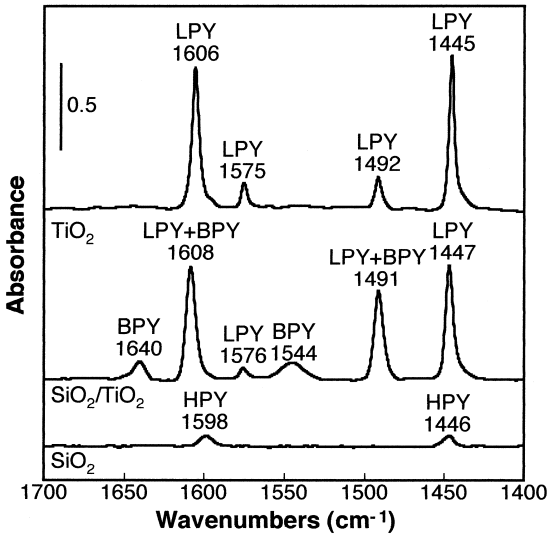

Fig. 2. Infrared spectra of pyridine adsorbed at 473 K on fresh SiO_2, SiO_2–TiO_2, and TiO_2. LPY: band corresponding to pyridine bonded to a Lewis acid site; BPY: band corresponding to pyridine bonded to a Brønsted acid site; and HPY: band corresponding to hydrogen-bonded pyridine.

with Ti^{4+} cations on the TiO_2 surface [37]. No evidence of hydrogen-bonded pyridine is observed. For pyridine adsorption on the binary oxide new bands are observed at 1640 and 1544 cm^{-1} indicating the presence of Brønsted acid sites. Evidence for Lewis acid sites is also present. The intensity of the peaks is related to the pyridine surface concentration at the experimental conditions. For pyridine adsorbed on SiO_2–TiO_2, the intensity of the bands for Lewis acid sites decreases slightly compared to the intensities observed for TiO_2 indicating that the concentration of Lewis sites decreases for the binary oxide. However, new Brønsted sites are generated and the overall number of acid sites does not seem to change significantly. Indeed, ammonia adsorption microcalorimetry experiments at 423 K have confirmed that the overall acidity is about the same for these samples [Pizarro-Crespo, Cardona-Martínez, unpublished]. The data presented above indicate that no pure metal oxide displays Brønsted acidity but when SiO_2 is cofumed with TiO_2, Brønsted acidity is generated. Our results are consistent with the work of Odenbrand and coworkers [37] who found equivalent results for similar samples. The new Brønsted acidity may have implications on the photocatalytic reactivity of the binary oxide as discussed below.

3.2. FTIR spectroscopy of adsorbed toluene

Fig. 3 shows the infrared spectra of toluene adsorbed at 300 K on fresh SiO_2, SiO_2–TiO_2, and TiO_2. These spectra correspond to the toluene remaining adsorbed on the sample after removing from the cell the gas-phase toluene and any weakly adsorbed toluene by flowing helium at room temperature. Note that the intensities of the bands for toluene adsorbed on the binary oxide are significantly higher than for the other samples. Since the same mass of metal oxide was used for all experiments, the SiO_2–TiO_2 seems to adsorb a significantly higher amount of toluene than TiO_2 at 300 K. Silica, on the other hand, has a small adsorption capacity for toluene. Apparently, the addition of SiO_2 to TiO_2 enhances the adsorption of toluene more than the adsorption of pyridine at 473 K or ammonia at 423 K. The enhancement appears to be the result of the generation of new surface sites that are different from those attributable to a mechanical mixing of the two materials.

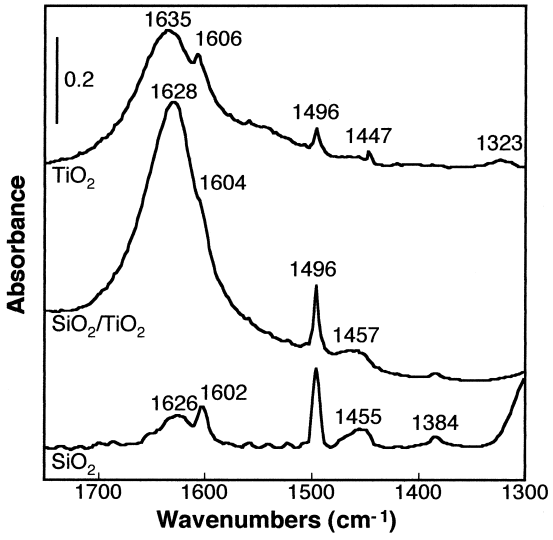

Fig. 3. Infrared spectra of toluene adsorbed at 300 K on fresh SiO_2, SiO_2–TiO_2, and TiO_2.

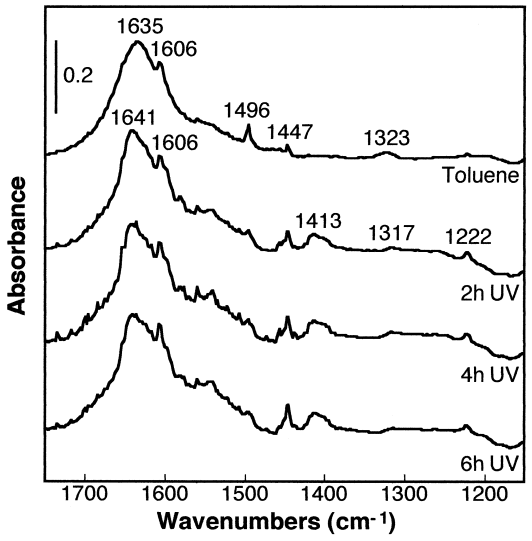

Fig. 4. Infrared spectra of toluene adsorbed at 300 K on fresh TiO_2 and after increasing irradiation times.

Toluene appears to adsorb molecularly on all samples with no significant changes from the gas-phase structure. The bands observed between 1635 and 1626 cm^{-1} and between 1606 and 1602 cm^{-1} are assigned to aromatic ring vibrations [34]. The band centered at 1496 cm^{-1} was observed at the same frequency for the three oxides indicating that it should correspond to a vibration of a functional group that does not interact with the surface, possibly the methyl group. This hypothesis was confirmed by adsorbing deuterated toluene ($C_6D_5CD_3$) over SiO_2–TiO_2. After adsorption of deuterated toluene only one band centered at 1632 cm^{-1} was observed in the region of interest supporting our assignment. Adsorption of a deuterated compound should displace the vibrations corresponding to C–H to lower vibrational frequencies, but should not change extensively the position of bands corresponding to C–C vibrations [38]. The results discussed above indicate that toluene adsorbs on TiO_2 or on SiO_2–TiO_2 through interaction with the aromatic ring.

After toluene adsorption, the samples presented in Fig. 3 were irradiated with UV light while flowing He in the absence of gas-phase O_2 and H_2O. Silica is not photocatalytically active for toluene oxidation and toluene is easily desorbed from the surface by heating or irradiating with a UV lamp with or without gaseous O_2 and/or H_2O. For TiO_2, irradiating the adsorbed toluene with UV light in flowing He seems to desorb a small fraction of the toluene without a significant formation of new surface species as can be observed in Fig. 4. Only a new small band centered at 1413 cm^{-1} is detected. The lack of photocatalytic activity of TiO_2 in the absence of gas-phase O_2 was confirmed with the fixed bed reactor. No significant conversion was observed while flowing toluene in nitrogen under UV radiation [Delgado-Cruz, Cardona-Martínez, unpublished].

For the SiO_2–TiO_2 photocatalyst, however, new surface species are formed when adsorbed toluene is irradiated with UV light in flowing He as shown in Fig. 5. New bands appear at 3072, 1684, 1646, 1599, 1582, 1457, 1417, and 1318 cm^{-1}. As the irradiation time is increased new bands appear at 1512 and 1451 cm^{-1}, and the band centered at 1417 becomes more intense. When a sample, that had been irradiated for 6 h, was heated at increasingly higher temperatures in flowing helium, the intensity of most bands decreased while the intensity of the bands centered at 1417, 1452, and 1512 cm^{-1} increased significantly. These results indicate that as the reaction progresses both weakly and strongly adsorbed surface species are formed. The most strongly adsorbed species are formed even thermally. Also, the addition of SiO_2

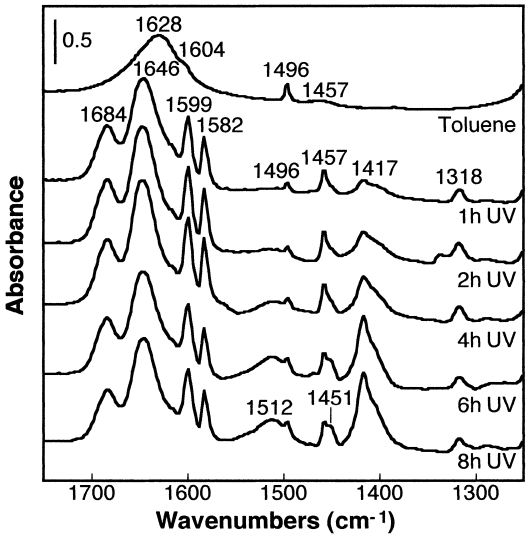

Fig. 5. Infrared spectra of toluene adsorbed at 300 K on fresh SiO_2–TiO_2 and after increasing irradiation times.

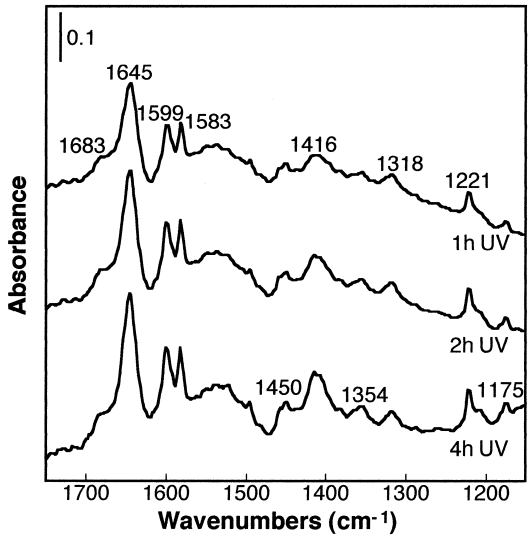

Fig. 6. Infrared spectra of adsorbed species on TiO_2 after the photocatalytic oxidation of 75 ppm toluene in air (WHSV= 383 h^{-1}).

to TiO_2 enhances the reactivity of the surface as compared to TiO_2. For the binary oxide significantly higher concentrations of surface products are observed even in the absence of gaseous oxygen. Two sources of oxygen might explain this result. The toluene could react with oxygen that remains adsorbed on the surface after the pretreatment or it is possible that the surface of the binary oxide is partially reduced during the reaction. For the last case the reaction would become stoichiometric under the present conditions, but if gas-phase oxygen is added to the reactive mixture it would reoxidize the surface completing the catalytic cycle.

3.3. *FTIR spectroscopy of surface species formed during the photocatalytic oxidation of toluene*

The behavior for TiO_2 is different when a mixture of 75 ppm toluene and oxygen is flowed over the catalyst while irradiating with UV light as depicted in Fig. 6. Under these conditions new bands located at 3069, 1683, 1599, 1583, 1450, 1416, 1318, and 1221 cm^{-1} are seen. As the irradiation time is increased the bands centered at 1450 and 1416 cm^{-1} become more intense. The results for SiO_2–TiO_2 are similar to those found without gas-phase O_2 as may be observed in Fig. 7. A comparison between Figs. 6 and 7 reveals

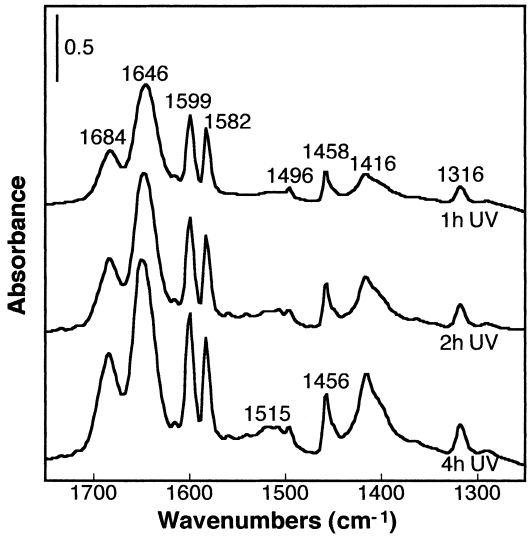

Fig. 7. Infrared spectra of adsorbed species on SiO_2–TiO_2 after the photocatalytic oxidation of 75 ppm toluene in air (WHSV= 372 h^{-1}).

once again that the intensity of the peaks observed for reaction over SiO_2–TiO_2 are significantly higher than those for TiO_2. This result indicates that the surface concentrations are also higher. Fig. 8 presents the effect of the time on stream (or irradiation time) on the toluene conversion in the absence of gas-phase

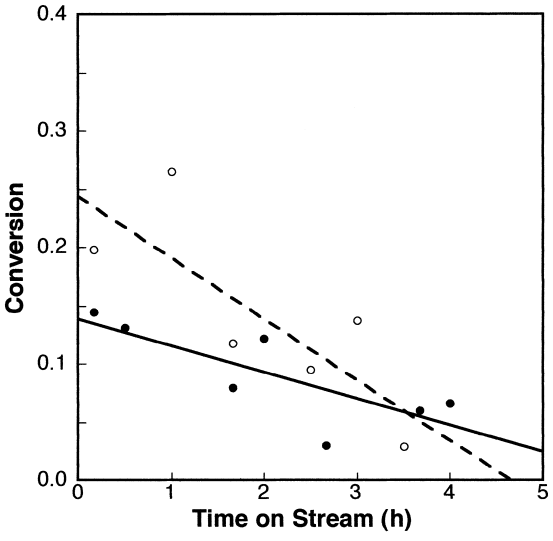

Fig. 8. Effect of time on stream on toluene conversion in the absence of gas-phase water ((– • –) TiO_2, WHSV=383 h^{-1};(– ○ –) SiO_2–TiO_2, WHSV=372 h^{-1}; inlet toluene concentration= 75 ppm).

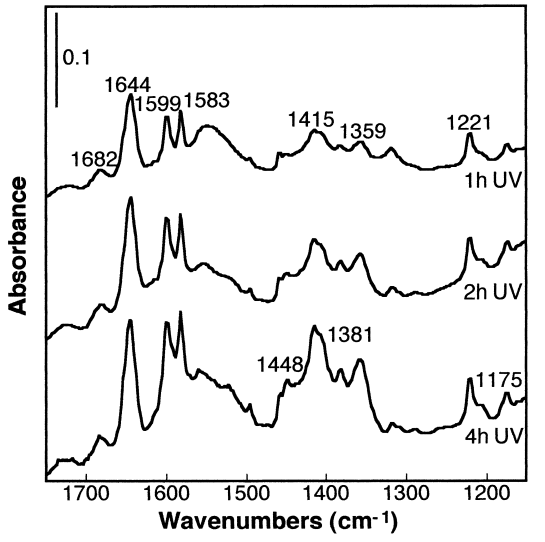

Fig. 9. Infrared spectra of adsorbed species on TiO_2 after the photocatalytic oxidation of 63 ppm toluene in air and 1200 ppm water (WHSV=479 h^{-1}).

water and at a weight hourly space velocity (WHSV) of about 380 h^{-1}. The conversion was calculated by measuring the inlet and outlet toluene concentrations with a GC/FID. These results were obtained in situ with the IR cell and correspond to the previously discussed experiments. Under these conditions the binary oxide is initially more active than TiO_2 and both photocatalysts deactivate with time on stream. Using the site density reported by Sauer and Ollis [19] we calculated the catalyst surface monolayer equivalents for our samples. For TiO_2, the number of monolayer equivalents for 1, 2, and 4 h of UV irradiation are approximately 0.5, 1.0, and 1.5 molecules converted per catalyst site, respectively. For the binary oxide the corresponding results are 1.0, 1.7, and 2.5 molecules converted per catalyst site, respectively. After 1 h in the case of SiO_2–TiO_2 and after 2 h in the case of TiO_2 we are in the region where Sauer and Ollis expect deactivation which is consistent with our observations. Part of the scatter observed in Fig. 8 may be attributed to partial desorption of surface species when removing the gas-phase toluene before collecting the spectra that cause an apparent increase in activity. The trends are obvious, however, and the differences are significant and reproducible. Looking collectively at Figs. 6–8 there is an apparent correlation between the deactivation of the photocatalysts and the intensification of the band centered around 1416 cm^{-1}. It seems that the surface species that causes this band might be responsible for the catalyst deactivation.

Figs. 9–11 show results equivalent to those described above but with about 60 ppm of toluene

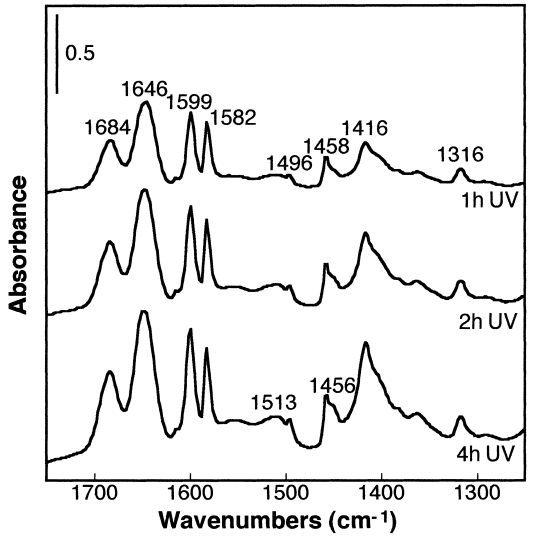

Fig. 10. Infrared spectra of adsorbed species on SiO_2–TiO_2 after the photocatalytic oxidation of 62 ppm toluene in air and 1200 ppm water (WHSV=799 h^{-1}).

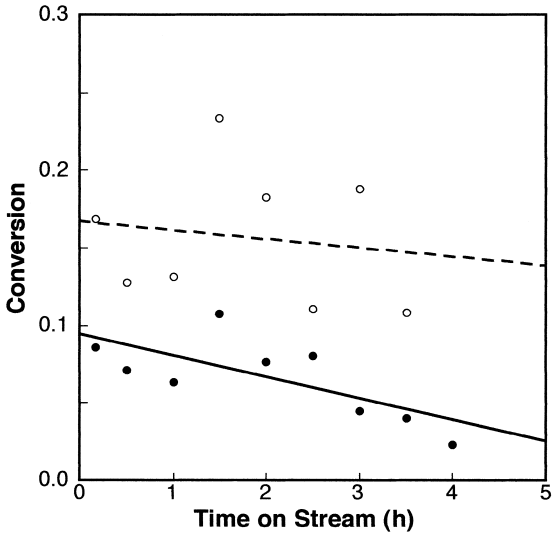

Fig. 11. Effect of time on stream on toluene conversion in the presence of gas-phase water ((– • –) TiO_2, WHSV=479 h^{-1}; (– ○ –) SiO_2–TiO_2, WHSV=799 h^{-1}; water concentration=1200 ppm).

and 1200 ppm of water vapor in the reactive mixture to test the effect of water on the oxidation of toluene. The spectra show the same bands observed before in about the same proportion. The main difference when compared with the previous spectra is that the intensity of all peaks is considerably smaller. Apparently, the presence of water slows the formation of the surface species. Two possible explanations may be given for this behavior. Perhaps the water competes for the sites where the species are formed or it partially regenerates the active sites. A comparison of the activity of the two photocatalysts shows that even with roughly half the residence time (WHSV=799 h^{-1} for SiO_2–TiO_2 compared to WHSV=479 h^{-1} for TiO_2) the conversion for the binary oxide is higher than for the single oxide. More importantly, SiO_2–TiO_2 retains most of it activity after 4 h of irradiation. This instance the monolayer equivalents, for the same times on stream as before, are 0.4, 0.8, and 1.3 molecules converted per catalyst site for TiO_2 and 1.1, 2.6, and 4.3 molecules converted per catalyst site for SiO_2–TiO_2. According to these results we would have expected that the binary oxide should have lost a significant fraction of its activity even after 1 h of UV irradiation, but this was not the case. Obviously, the presence of water is slowing the deactivation of this sample. For TiO_2 the effect is not as clear because we do not get to one monolayer equivalent until about 2.5 h of irradiation. A more controlled study using the fixed bed reactor is currently under way to try and understand more quantitatively these effects.

Table 1
Assignment of IR bands

Wave numbers (cm^{-1})	Functional group	Reference
1686–1681	C=O of an aldehyde	[35,36]
1650–1641	C=C of aromatic ring	[34]
1601–1599	C=C of aromatic ring	[34]
1584–1582	C=C of aromatic ring	[34]
1417–1413	Interaction between the C–O and O–H of carboxylic acid	[34]
1318–1316	Weak absorption of aromatic aldehyde	[34]

An analysis of the most important bands discussed above induced us to assign those bands to the functional groups summarized in Table 1. From this analysis we may conclude that two possible surface species generated during the photocatalytic oxidation of toluene are an aromatic aldehyde and a carboxylic acid. In addition, GC analysis of the gas-phase products identified traces of benzaldehyde as the only organic compound formed. Therefore, benzaldehyde and benzoic acid are potential candidates for the partial oxidation surface products observed in this study.

Figs. 12 and 13 show spectra for adsorption of benzaldehyde and benzoic acid on the fresh photocatalysts. These spectra are compared to the spectra obtained after 1 and 10 h of photocatalytic oxidation of toluene, respectively. Benzaldehyde adsorption produced spectra that were nearly identical to those corresponding to the initial period of UV irradiation. Further irradiation of the samples with adsorbed benzaldehyde yielded spectra analogous to those corresponding to the deactivated samples. These results demonstrate that toluene is initially partially oxidized to benzaldehyde on the surface of the photocatalysts. Benzaldehyde is then further oxidized into the strongly adsorbed surface species that is responsible for the deactivation of the photocatalyst. The most intense bands observed after adsorption of benzoic acid on the fresh photocatalysts coincides with the bands that intensify as the catalysts deactivate. This

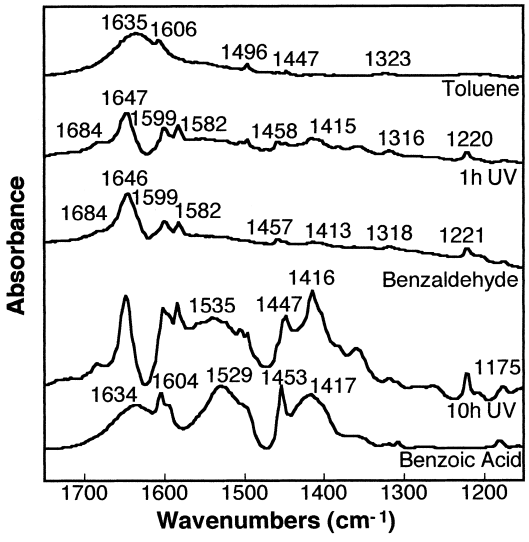

Fig. 12. Infrared spectra of TiO_2 surface after adsorption of toluene, benzaldehyde, or benzoic acid, or after photocatalytic oxidation of toluene.

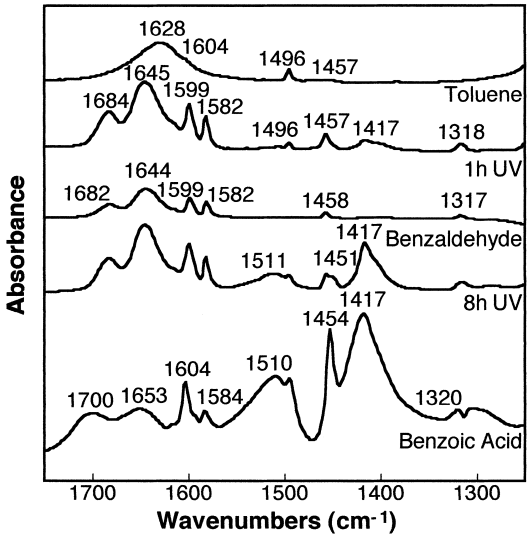

Fig. 13. Infrared spectra of SiO_2–TiO_2 surface after adsorption of toluene, benzaldehyde, or benzoic acid, or after photocatalytic oxidation of toluene.

result supports the conclusion that this seems to be the surface species responsible for the deactivation.

To confirm our identification we performed a methanol extraction of the adsorbed species present on the deactivated photocatalysts followed by GC/MS analysis. This analysis identified benzaldehyde, benzyl alcohol, and benzoic acid in the solution. The concentrations found for the binary oxide were higher than those for the single oxide. This is consistent with our interpretation of the differences in intensity of the IR bands for the single and binary oxide. The relative concentrations of benzoic acid were small compared to the other species, in particular for TiO_2. Apparently, methanol is not an efficient solvent to extract benzoic acid from these surfaces. Significantly longer extraction times were required for the TiO_2 samples. This result may imply that the species are more strongly adsorbed on this oxide or that, since the concentrations are lower, additional time is required to be able to detect the compounds.

The GC/MS results confirmed our original conclusion but also identified an additional surface species, benzyl alcohol. Room temperature adsorption of benzyl alcohol produces the spectra shown in Figs. 14 and 15 compared to the results after 4 h of irradiation. Since the position of the most intense bands coincide with some bands observed for the other compounds and the relative surface concentration of benzyl alcohol was smaller, identification using FTIR is not as conclusive as for the other compounds. Fig. 15 also shows a spectrum after irradiation of adsorbed benzyl

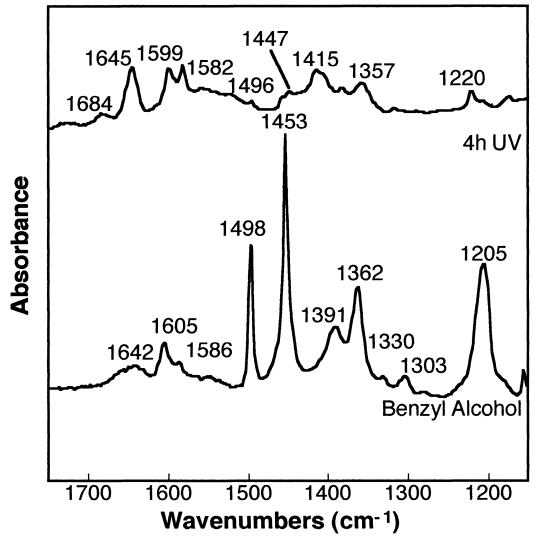

Fig. 14. Infrared spectra of TiO_2 surface after 4 h of photocatalytic oxidation of toluene and after adsorption of benzyl alcohol.

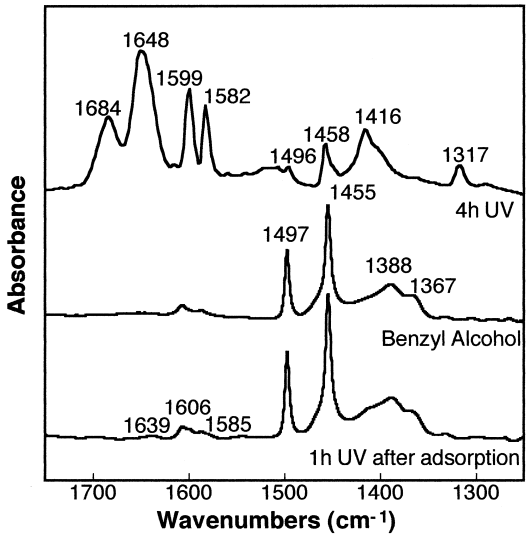

Fig. 15. Infrared spectra of SiO_2–TiO_2 surface after 4 h of photocatalytic oxidation of toluene, after adsorption of benzyl alcohol, and after 1 h of UV irradiation after benzyl alcohol adsorption.

alcohol while flowing air over the catalyst and this time no significant change was observed. The apparently low reactivity of benzyl alcohol is not clearly understood and additional tests will be performed to check this result.

4. Conclusions

Using in situ FTIR spectroscopy we have identified the main partial oxidation products formed on the surface of TiO_2 and 8% SiO_2–TiO_2 during the photocatalytic oxidation of toluene. During the initial stages of the reaction benzaldehyde is the preferential surface species formed. As the time on stream or irradiation time increases the benzaldehyde is further oxidized into benzoic acid that accumulates on the surface. Benzoic acid is strongly adsorbed on the surface of the catalyst. The accumulation of benzoic acid on the surface appears to be responsible for the catalysts deactivation. The presence of gas-phase water in the reactive mixture seems to retard the formation of benzoic acid.

Additional GC/MS analysis of methanol-extracted surface species confirmed the presence of benzaldehyde and benzoic acid and detected small concentrations of benzyl alcohol. This species appears to be less reactive than either toluene or benzaldehyde and seems to be formed at a lower rate.

The SiO_2–TiO_2 photocatalyst is more active and appears to deactivate slower than TiO_2, specially in the presence of water vapor. The surface of the binary oxide is reactive even in the absence of gas-phase oxygen. It also seems to have a higher toluene adsorption capacity than TiO_2. The acidity of the different oxides was examined using FTIR spectroscopy of adsorbed pyridine. The results indicate that no pure metal oxide displays Brønsted acidity but when SiO_2 is cofumed with TiO_2, Brønsted acidity of intermediate strength is generated. The generation of new surface sites may be responsible for the increased activity. The mechanism of this promotion effect is not clearly understood and further studies are required to elucidate it.

Acknowledgements

The research presented here was accomplished under the financial support of the Department of Energy-EPSCoR Program Grant (GN DE-FG02-94ER75764). In addition, we wish to thank the University of Puerto Rico – Mayagüez Campus (UPR–RUM) for the partial support to one of us (RMR). Furthermore, we wish to acknowledge the technical support provided by the UPR–RUM Chemical Engineering Department (in particular Mr. Angel Zapata, Dr. José A. Colucci, and Edna Delgado). Finally, we appreciate the help provided by the Degussa for providing the photocatalysts samples used in this work and Mobil Research and Development for donating part of the hardware used.

References

[1] M.R. Hoffmann, S.T. Martin, W. Choi, D.W. Bahnemann, Chem. Rev. 95 (1995) 69.
[2] A.L. Linsebigler, G. Lu, J.T. Yates, Chem. Rev. 95 (1995) 735.
[3] O. Legrini, E. Oliveros, A.M. Braun, Chem. Rev. 93 (1993) 671.
[4] D.F. Ollis, H. Al-Ekabi (Eds.), Photocatalytic Purification and Treatment of Water and Air, Elsevier, Amsterdam, 1993.
[5] L.A. Dibble, G.B. Raupp, Catal. Lett. 4 (1990) 345.

[6] L.A. Dibble, G.B. Raupp, Environ. Sci. Technol. 26 (1992) 492.
[7] L.A. Phillips, G.B. Raupp, J. Mol. Catal. 77 (1992) 297.
[8] M.R. Nimlos, W.A. Jacoby, D.M. Blake, T.A. Milne, Environ. Sci. Technol. 27 (1993) 732.
[9] E. Berman, J. Dong, Proceedings of the Third International Symposium on Chemical Oxidation Technology for the Nineties, Vanderbilt University, Nashville, Tennessee, 17–19 February 1993.
[10] C.S. Turchi, E.J. Wolfrum, M. Nimlos, Proceedings of the Fifth Annual Symposium on Emerging Technologies in Hazardous Waste Management, I&EC Special Symposium, American Chemical Society, Atlanta, GA, 27–29 September 1993.
[11] C. Lyons, C. Turchi, D. Gratson, Proceedings of the 88th Annual Symposium Meeting and Exhibition of the Air and Waste Management Association, San Antonio, TX, 18–23 June 1995.
[12] M.L. Sauer, M.A. Hale, D.F. Ollis, Photochem. Photobiol. A 88 (1995) 169.
[13] Y. Luo, D.F. Ollis, J. Catal. 163 (1996) 1.
[14] S.A. Larson, J.L. Falconer, Catal. Lett. 44 (1997) 57.
[15] T. Ibusuki, K. Takeuchi, Atmos. Environ. 20 (1986) 1711.
[16] J. López, M.S. Thesis, University of Puerto Rico – Mayagüez, 1996.
[17] T.N. Obee, R.T. Brown, Environ. Sci. Technol. 29 (1995) 1223.
[18] R. Méndez-Román, M.S. Thesis, University of Puerto Rico – Mayagüez, 1996.
[19] M. Sauer, D.F. Ollis, J. Catal. 163 (1996) 215.
[20] J. Cunningham, B.K. Hodnett, J. Chem. Soc. Faraday Trans. 1(77) (1980) 2777.
[21] J. Peral, D.F. Ollis, J. Catal. 136 (1992) 554.
[22] S.A. Larson, J.L. Falconer, Appl. Catal. B 4 (1994) 325.
[23] W. Jacoby, D.M. Blake, J.A. Fennell, J.E. Boulter, L.M. Vargo, M.C. George, S.K. Dolberg, J. Air & Waste Manage. Assoc. 46 (1996) 891.
[24] C. Anderson, A.J. Bard, J. Phys. Chem. 99 (1995) 9882.
[25] F. Xinazhi, L.A. Clark, Q. Yang, M.A. Anderson, Environ. Sci. Technol. 30 (1996) 647.
[26] N. Takeda, T. Torimoto, S. Sampath, S. Kuwabata, H. Yoneyama, J. Phys. Chem. 99 (1995) 9986.
[27] DE-PS 870 242 Degussa, 1941.
[28] M. Ettlinger, Highly Dispersed Metallic Oxides Produced by the AEROSIL® Process, Technical Bulletin Pigments No. 56, Degussa, Germany, 1993.
[29] N. Cardona-Martínez, J.A. Dumesic, J. Catal. 125 (1990) 427.
[30] G. Connell, Ph.D. thesis, University of Wisconsin – Madison, 1985.
[31] P. Pichat, M.-V. Mathieu, B. Imelik, Bull. Soc. Chim. Fr. 8 (1969) 2611.
[32] C.H. Kline, J. Turkevich, J. Chem. Phys. 12 (1944) 300.
[33] F.A. Diaz-Mendoza, L. Pernett-Bolãno, N. Cardona-Martínez, Thermochim. Acta 312 (1998) 47.
[34] G. Socrates, Infrared Characteristic Group Frequencies, Wiley, New York, 1980.
[35] S. Tunesi, M.A. Anderson, Langmuir 8 (1992) 487.
[36] H. Sun, F. Blatter, H. Frei, J. Am. Chem. Soc. 116 (1994) 7951.
[37] C.U. Odenbrand, G.M. Brandin, G. Busca, J. Catal. 135 (1992) 505.
[38] H. Ibach, J.E. Müeller, in: M.L. Deviney, J.L. Gland (Eds.), Catalyst Characterization Science Surface and Solid State Chemistry, American Chemical Society, Washington, DC, 1985, p. 392.